https://doi.org/10.5194/amt-2022-216
Preprint. Discussion started: 20 July 2022

Atmospheric Measurement Techniques Discussions

A High-Resolution Record of Ice Nuclei Concentrations Between -20 to -30 °C for Fall and Winter at Storm Peak Laboratory with the autonomous Continuous Flow Diffusion Chamber Ice Activation Spectrometer

Anna L. Hodshire[1], Ezra J. T. Levin[1], A. Gannet Hallar[2], Christopher N. Rapp[3], Dan R. Gilchrist[2], Ian McCubbin[2], Gavin R. McMeeking[1]

[1] Handix Scientific Inc., Fort Collins, CO, 80526, USA
[2] Department of Atmospheric Sciences, University of Utah, Salt Lake City, UT, 84112, USA
[3] Department of Earth, Atmospheric, and Planetary Sciences, Purdue University, West Lafayette, IN, 47907, USA

Correspondence to: Anna L. Hodshire (anna@handixscientific.com)

Abstract. Ice nucleating particles (INPs) influence the timing and amount of precipitation in mixed-phase clouds by acting as seeds for supercooled liquid droplets to form ice upon. High-resolution, long-term measurements of ice nucleating particles (INPs) have been impeded by complex instrumentation that requires a trained on-site technician to operate or analyze offline. We have significantly updated the well-characterized continuous flow diffusion chamber (CFDC) instrument to run autonomously with minimal in-person handling and easy remote access. This new CFDC, the CFDC-Ice Activation Spectrometer (CFDC-IAS) was deployed for four months (October 2020-January 2021) at the mountain-top Storm Peak Laboratory site in Colorado and provided 5-minute resolution measurements daily at target temperatures of -20, -25, and -30 °C. Concentrations of INPs across all temperatures had a median value of 6 per standard liter (sL^{-1}), and a mean of 10 sL^{-1} with a range of ~0-470 sL^{-1}. The CFDC-IAS was served once a week by a technician who changed out diffusion dryer desiccant and replaced the nitrogen tank as needed, and otherwise was operated remotely for desired changes in the sampling routine.

1 Introduction

Ice nucleating particles (INPs) have significant impacts on mixed-phase clouds through altering of precipitation processes and radiative properties (DeMott et al., 2010). High-resolution, long-term measurement records of INPs are currently scarce due to the difficulty of making INP measurements. Unlike measurements of some other important aerosol characteristics, such as composition (Ng et al., 2011) or cloud condensation nuclei (Schmale et al. 2018), real-time ambient INP measurement techniques typically require an experienced technician on-site, and usually only occur in the context of intensive field campaigns (Lacher et al., 2018). The majority of single-site, longer-term (one year or longer) continuous records of INP require off-line processing and typically have daily to weekly time resolutions (Schneider et al., 2021) or may only capture short

https://doi.org/10.5194/amt-2022-216
Preprint. Discussion started: 20 July 2022


Atmospheric Measurement Techniques Discussions

periods of each day, such as an hour or a few hours (Schrod et al., 2020b; Müller, 1969a). As discussed in (Schrod et al., 2020b), many successful longer-term records of INP occurred in the 1950s-1970s (Soulage, 1966; Kline, 1963; Bigg and Miles, 1964; Bigg, 1973; Müller, 1969b). Only recently have high-resolution, longer-term measurements been achieved with INP measurements (Möhler et al. 2021; Brunner and Kanji 2021). Limited understanding of how rapidly changing global emissions including anthropogenic sources may impact INP and associated radiative forcings (Schrod et al., 2020a; Boucher et al., 2013) along with limited spatial and temporal resolution of INP globally points to the importance of more frequent INP measurements.

Here, we have deployed a new continuous flow diffusion chamber (CFDC), the Handix Scientific CFDC-Ice Activation Spectrometer (CFDC-IAS) for four months (October 2020-January 2021) at the mountaintop Storm Peak Laboratory (SPL) in Steamboat Springs, CO (3220 m above mean sea level). The CFDC-IAS is based on the well-characterized Colorado State University CFDC (DeMott et al., 2015; Rogers et al., 2001) but has undergone significant modifications to allow for automated and near-continuous operation. The four-month, high-resolution mountaintop time series provides INP concentrations between -20 to -30 °C and follows a successful month-long deployment in May-June 2018 of an earlier version of the CFDC-IAS in Beijing, China (Bi et al., 2019). The purpose of this Technical note is to introduce improvements made to the CFDC-IAS and provide an overview of the data collected in context to previous INP analyses and parameterizations (e.g. (Niemand et al. 2012; DeMott et al. 2010; DeMott et al. 2015; Bi et al. 2019; Lacher et al. 2018).

2. Methods

2.1 The CFDC-IAS

The Handix Continuous Flow Diffusion Chamber Ice Activation Spectrometer (CFDC-IAS) deployed at SPL builds upon several decades of development of CFDC instruments for measuring ice nuclei concentrations. The CFDC-IAS is modeled after the well-characterized Colorado State University CFDC (Rogers et al. 2001; DeMott et al. 2015) with numerous updates to improve operability and automation. The basic design consists of a cylindrical chamber, with two concentric, ice-covered walls that particles pass between in a laminar flow. Establishing a temperature difference between the colder (inner) and warmer (outer) walls in the upper region of the chamber leads to an approximately steady-state region of water vapor and temperature. Any INPs that can activate at the conditional water vapor and temperature grow into ice crystals. The inner and outer walls of the lower region of the chamber are set to the same temperature to evaporate water droplets and wet aerosol while retaining the ice crystals from activated ice nuclei. The ice crystals are detected at the bottom of the chamber with an optical particle counter. Impactors upstream of the chamber have a 2.5 µm size cut to remove large particles that could be incorrectly optically classified as ice crystals, so the CFDC-IAS is designed to measure INP less than 2.5 µm in aerodynamic diameter.

https://doi.org/10.5194/amt-2022-216
Preprint. Discussion started: 20 July 2022


Atmospheric Measurement Techniques Discussions

The fundamental objective when preparing a CFDC for measurements is to apply a uniform coating of ice on both walls to a consistent height near the top of the chamber while minimizing the formation of frost on the interior surfaces that can cause background counts to be high. When operating, the objective is to maintain the desired measurement conditions while minimizing background counts and thereby maximizing the sensitivity to detecting INP. A major advantage of the software-controlled features developed for the CFDC-IAS is its ability to perform all setup and operational procedures through automatic sequence structures pre-built into the acquisition software. The sequence first prepares the chamber for measurement by pulling a vacuum on the column to remove any liquid water or water vapor that could form frost. It then cools the walls to a set temperature (typically -27 C) and then pumps water into the column, where it freezes and forms the ice layer. The amount of water pumped into the column is monitored with a water level sensor in the supply tank to ensure a consistent fill volume, and thus consistent ice wall length. Water for the ice layer is stored in a 5 L supply tank and while a small amount of water is lost over time to growing droplets and ice crystals, additional supply water was not necessary during the SPL deployment. Once the ice walls have been formed and excess water drained from the column, the instrument automatically adjusts the wall temperatures to achieve the user-set measurement conditions and begins sampling. Over time, typically ~6 hours, the ice walls will begin to deteriorate, leading to higher instrument background and reduced sensitivity. Thus, after a set sampling period, the instrument automatically warms the walls to melt the remaining ice and repeats the cycle.

The first CFDC-IAS was deployed in Beijing, China for one month (Bi et al., 2019) and updates from the CSU CFDC design to improve operability and automation are thoroughly described in that manuscript. This CFDC-IAS instrument has incorporated further updates. Most significantly the column material was changed from copper to anodized aluminum, while keeping the internal dimensions identical. The previous copper column design required chemical treatment (ebonization) to make the surface wettable and ensure a smooth ice layer. Over time, the surface layer would break down, leading to patchy ice layers that contributed to increasingly higher instrument backgrounds and more frequent “frost spikes”, requiring the surface to be retreated. This process was highly time consuming, requiring the entire instrument to be disassembled yearly, and required use of caustic chemicals. The aluminum column does not require this treatment, and we observed no background degradation during this study. To ensure that changing the column material did not alter the instrument's function, we compared the new column to the CSU-CFDC, which uses the copper design, and found good agreement between the two instruments for laboratory measurements (Figure 1). Additionally, the aluminum column was disassembled after the deployment to SPL and no visible change in the aluminum surface or its wettability was observed.

To account for spurious ice crystal counts originating from chamber surface frost, the CFDC-IAS switched between sampling HEPA filtered air and ambient air in 5-minute intervals. We determine INP concentrations by following the statistical methods laid out in the supplemental material of (Barry et al., 2021), which models INP counts in filter and sample periods as Poisson distributions. First a Poisson distribution rate parameter (lambda) is found:

https://doi.org/10.5194/amt-2022-216
Preprint. Discussion started: 20 July 2022


Atmospheric Measurement Techniques Discussions

$$\lambda_i = \frac{x_i}{n_i} \quad (1)$$

Statistically significant INP values are determined by using moment based statistics to identify if a sample rate parameter is significantly greater than the filter rate parameters directly before and after the sample period. Finally, the filter-corrected INP concentration (N_{INP}) is determined by

$$N_{INP} = \frac{\lambda_{sample} - \lambda_{filter}}{\underline{v}_{sample}} \quad (2)$$

where $\underline{v}_{sample}$ is the average flow rate over the sample time period (SL s^{-1}). From these calculations, 34% of the SPL CFDC-IAS data was determined to not be statistically higher than background. Here, we only present INP concentrations from sample periods determined to be statistically higher than background. The residence time for a particle in the chamber between the time that it activates to when it evaporates is nominally 5 s, but studies indicate the aerosol lamina may broaden in similar instruments, leading to longer residence times (Garimella et al., 2016). The broadening of the lamina along with other factors lead to higher supersaturations required in the CFDC to agree with expansion cloud chamber measurements. An underestimate of a factor of 3 is found for CFDC measurements of mineral dust INPs at a water relative humidity of 105% (DeMott et al., 2015). Here we do not apply any correction factor to the SPL CFDC-IAS data, as there is currently a lack of measurements that bound the uncertainty under different sampling conditions, but note that a correction of a factor of three or higher could be appropriate. While this correction appears to be a large difference, it is well within general uncertainties of ice nuclei measurements (DeMott et al., 2017).

At SPL, the CFDC-IAS sampled from the main aerosol inlet (Petersen et al., 2019). The inlet geometry and flow path for this instrument are the same as previous versions of the CFDC. In the lab we have measured losses of ~10% for particles less than 2.5 μm in diameter (e.g.Prenni et al. 2009). Sample air was drawn through two diffusion driers (Handix Scientific) filled with silica gel and molecular sieves, respectively, and then passed through a 2.5 um size cut impactor. Although the SPL inlet can transmit particles with an aerodynamic diameter up to 13 μm, only particles smaller than 2.5 μm can make it through the CFDC-IAS inlet. Thus we assume that during cloud or precipitation events we were primarily sampling the interstitial aerosol. The instrument was set to automatically melt the ice walls and then refreeze the walls after 4-6 hours of operation, as the instrument background begins to increase due to frost buildup on interior surfaces after several hours of operation, lowering the detection limit. The variability in sampling time was based on the number of temperature setpoints for each measurement cycle, with more setpoints leading to a longer sample cycle. During the SPL deployment, instrument operation time was almost evenly split between atmospheric measurements (31%), filter measurements (37%), and defrosting/refreezing intervals (33%). While the amount of time needed to refresh the ice layer is relatively fixed, the split between filter and sample measurement time is a user setting. For this field campaign we chose to set both the filter and sample periods to 5 min as we were interested in both the ambient measurements as well as changes in instrument function over time (the slightly longer percentage of time on filter was because the inlet was set to "Filter" when changing sampling temperatures). Instrument background concentrations were on average less than 1 L^{-1} at STP (denoted sL) at the beginning of an operation period and steadily

https://doi.org/10.5194/amt-2022-216
Preprint. Discussion started: 20 July 2022


Atmospheric Measurement Techniques Discussions

increased, occasionally reaching average concentrations of 2-12 sL^{-1}. As INP concentrations decrease at warmer temperatures (fewer particles activate) and can be as low as <1 sL^{-1}, we aligned the sampling temperatures to be sequentially at -20, -25, and -30 °C in approximately 2-hour cycles with warmest temperatures occurring at the start (cleanest background) of each operation cycle. Measurements taken during instrument transition periods when temperatures and/or saturation conditions were unstable were omitted from this analysis. The instrument operated continuously from October 10 2020-January 29 2021, except for January 3-10 due to a lack of nitrogen gas availability at the laboratory, which is used during the icing process to ensure no water vapor enters the chamber. A technician visited the site weekly to change out desiccant in the diffusion driers and switch nitrogen tanks when necessary (~every three weeks). Other than these visits, the instrument operated unattended during the measurement period.

2.2 Measurement location

The Storm Peak Laboratory (SPL) (40.455 deg N, -106.744 deg W) is located near Steamboat Springs, CO on the Steamboat Ski and Resort Corporation (SSRC) ski area at 3220 m above mean sea level. Steamboat Springs is located in the northwestern Colorado Rocky Mountains, and SPL is approximately 1150 m above and to the east of the town of Steamboat Springs and the Yampa Valley, an agriculture area (Borys and Wetzel, 1997). SPL is located on a 70 km-long north-south mountain barrier, oriented perpendicular to the prevailing westerly winds. The nearest large population center to the west of SPL is the Salt Lake Valley, approximately 430 km away. The climate of SPL is alpine, just above tree line, with dominant vegetation of Engelmann spruce, aspen, grasses, and flowering plants (Amin et al., 2013, 2012). The majority of precipitation for the area falls as snow between November and May. While snowfall on the SSRC ski area is highly variable from year to year, observations mid-mountain (455 m below SPL) reported an annual average of 287 inches (7289 mm) between the 2012-2021 seasons (https://www.onthesnow.com/colorado/steamboat/historical-snowfall; Colton et al., 2008). Air masses at SPL generally transition between nightly free-troposphere and daily boundary layer air (Obrist et al. 2008). A number of long-term meteorological and atmospheric state instruments are located at SPL, with guest instruments such as the Handix CFDC-IAS able to make shorter-term measurements. Further details on SPL are found in Borys and Wetzel (1997).

2.3 Supporting measurements, calculations, and modeling

SPL houses a number of meteorological and aerosol measurements that we use in this study for further INP concentration analysis. Meteorological data are hosted by the University of Utah MesoWest program (https://mesowest.utah.edu/), and include temperature, pressure, relative humidity, and wind speed and direction, all at 5-minute resolution. The wind direction was reported by cardinal direction (north, north-northeast, and so forth). A scanning mobility particle spectrometer (SMPS) measured aerosol from 10-350 nm at 5-minute resolution (Gannet Hallar et al., 2016) while an aerodynamic particle sizer (APS) measured aerosol from 0.55-20 µm at 5-minute resolution (Hallar et al., 2011). The SMPS and APS data were combined to calculate total aerosol surface area between 10 nm - 2.5 µm, assuming spherical particles. As there was no overlap in size range, we used the full ranges of both instruments. The APS aerodynamic diameters were further converted to volumetric

https://doi.org/10.5194/amt-2022-216
Preprint. Discussion started: 20 July 2022


Atmospheric Measurement Techniques Discussions

diameters following (DeCarlo et al., 2004). Particle surface area was used in calculating surface active site density, n_s, (Niemand et al., 2012; Connolly et al., 2009) found by dividing the INP concentrations ($n_{INP}(T)$) by aerosol surface area (S_{tot}):

$$n_s = n_{INP}(T) * \frac{10^9}{Stot} \quad (3)$$

With S_{tot} in units of μm^2 per unit volume of air, $n_{INP}(T)$ in units of sL^{-1} per unit volume of air, and n_s in units of m^{-2}.

We calculate 5-day back trajectories using the NOAA HYSPLIT on-line READY model (Stein et al., 2015; Draxler and Hess, 1998, 1997; Rolph et al., 2017), using 1-degree GDAS reanalysis meteorological data, starting each run at 500 m above model ground level.

3. CFDC-AIS Measurements at the Storm Peak Laboratory & Discussion

3.1 Stability and performance of the CFDC-IAS

The CFDC-IAS at SPL ran continuously between October 9, 2020 and January 29, 2021, except for January 5-10 (Figure 2), when the nitrogen tank ran out before a technician could visit. Most days the instrument was set to measurement cycles of target laminar temperatures of -20, -25, and -30 °C (target laminar water supersaturations of 3, 4, and 5%; Figure 3). Periodically, the instrument was instead set to run at only -30 °C to test instrument performance at one temperature, including between October 22 to November 8, 2020, November 19 to December 4, 2020, December 13 to December 25, 2020, and January 2 to January 5 2021. The instrument was able to reach the target temperatures to within 0.3°C and the target water supersaturations to within 3%. During measurement cycles, the average difference between inner and outer wall temperatures were ~15 °C (Figure 3). Two-hour replenishment cycles to thaw and reice the chamber walls occurred every four to six hours, depending on the preset measurement cycle. Periodically, the instrument was set to run only at -30 °C to better observe changes in INP concentrations without changing measurement conditions. All changes to the measurement cycles were done remotely.

3.2 INP concentrations, comparisons to previous SPL and other mountaintop measurements, and parameterizations

Concentrations of INPs found to be statistically higher than background had a median of 6 sL^{-1} and mean of 10 sL^{-1} across all temperature ranges (-20, -25, and -30 °C) (Figure 2 and 4), but with large variation (~0-470 L^{-1}). Coincidentally, some of the cleanest periods of the campaign happened during times that the CFDC-IAS was run only at -30 °C, leading to the apparent contradiction of -30 °C measurements including the lowest INP measurements (Figure 4a). Little (<10%) difference in medians or interquartile ranges occurred for observations taken in cloud (observations at >90% RH) versus out of cloud (Figure S1). Observations taken during the day had a lower mean INP concentration than observations taken at night (9.8 sL-1 versus 12 sL-1 ; Figure S1), but still had similar interquartile ranges (<20% different) between daytime and nighttime observations. Nighttime has previously been characterized as a rough proxy for free tropospheric air masses at SPL due to the presence of lower water vapor, aerosol, ozone, and CO concentrations (Obrist et al., 2008). Snowfall occurred at SPL on 35 of the 111-

https://doi.org/10.5194/amt-2022-216
Preprint. Discussion started: 20 July 2022


Atmospheric Measurement Techniques Discussions

day measurement period, while winds came primarily from the west (Figure 2). Ambient temperature at SPL ranged from -22.5 to 14.5 °C (mean -6.8 °C, median -8 °C) and ambient wind speed ranged from 0.7-55.3 mph (mean 16.4 mph, median 15.9 mph). No strong correlation (correlation coefficient > 0.8; Evans 1996) between snowfall, temperature, relative humidity, wind direction, or wind speed and INP concentrations were observed. Periodic high (>50 sL^{-1}) concentrations of INP followed periods of air parcels arriving from both surrounding arid regions and oceanic regions as determined by 5-day HYSPLIT back trajectories, including southeastern Wyoming, Nevada, Arizona, the Four Corners region, the Gulf of California, and the north Pacific (Figure S2). However, low concentrations of INP during the campaign were also observed to have similar back trajectories, including days before or after high INP event days (Figure S3), limiting our conclusions on the direct sources of INP to SPL. We do not include an analysis of precipitation along the back trajectories here but this could be an area of further research, as previous studies indicate that precipitation can either increase or decrease INP concentrations (Stopelli et al. 2015; Huffman et al. 2013; Mignani et al. 2021). The lack of temperature dependence on INP concentrations (Figure 4a) may be indicative of the dominance of warm-temperature INP types such as biological particles (Murray et al. 2012) during the measurement period that generally activate by -20 °C. The SPL measurement campaign did not include dedicated filter samples that could be analyzed off-line to determine the specific INP types. We suggest that the combination of a high-resolution INP record from a CFDC or similar instrument along with a lower-resolution filter sample record could allow for the combined analyses of temporal INP variability and INP speciation.

Previous CFDC deployments to SPL found average INP concentrations between -5 and -50 °C to be 1-10 sL^{-1} for both November 2001 and April-March 2004 (Richardson et al., 2007; DeMott et al., 2003), similar to our observations. However, of the ranges reported in these studies, our range of INP at SPL reached higher concentrations. Other high-elevation INP measurements also tend to fall within <1-10 sL^{-1}, with some sites reaching ~20-30 sL^{-1} (Lacher et al., 2018). The discrepancy in maximum concentrations observed between our study and other SPL and high-elevation studies may be due to differences in sampling frequency and duration: our measurements provide better temporal coverage than previous measurements at SPL, increasing the likelihood that we would be able to capture short-term, high-concentration events. As well, the high-elevation measurements in (Lacher et al. 2018) focus on free-troposphere measurements while we do not have available measurements to definitively state when we are in or out of the free troposphere and instead only estimate that nighttime measurements are likely to be in the free troposphere. The SPL nighttime-only median INP concentrations were 17% higher than the campaign median of 6 sL^{-1}, at 7 sL-1, still well within the range of (Lacher et al. 2018). Other factors that can lead to differences in observations from study to study include ambient conditions, such as precipitation and weather patterns as well as substantial increases in drought severity and locations across the Western U.S. between autumn of 2001 and autumn-winter of 2020-2021 (U.S. Drought Monitor, https://droughtmonitor.unl.edu/Maps/MapArchive.aspx).

Previous INP laboratory and field efforts have found relationships between total aerosol surface area or aerosol concentrations above 500 nm and INP concentrations for specific species of INP, such as dust (Niemand et al., 2012; DeMott et al., 2010, 2015). Total aerosol surface area (calculated as the sum of surface areas from the APS and SMPS; Methods) and aerosol

https://doi.org/10.5194/amt-2022-216
Preprint. Discussion started: 20 July 2022


Atmospheric Measurement Techniques Discussions

concentrations for the APS and SMPS are shown in Figure 2. The APS data represents the aerosol concentrations above 500 nm and can have an outsized influence on surface area, as larger particles can dominate aerosol surface area, when present. The APS counts were generally very low (1 or less). Periodic increases in APS counts were observed (Figure 2), generally during periods of winds between the west-southwest and the north-northeast (Figure 2). Surface active site density, n_s, (eq. 1) also referred to as ice-active surface site density, is the sites upon which ice can form per surface area of a specific INP type that are active at temperature T. Currently, n_s is only strictly valid for describing a single type of INP. We follow (Bi et al., 2019; Levin et al., 2019) in comparing our results to previous values of n_s to further diagnose the type of INPs that may have been present at SPL (Figure 4). Median values of n_s were 4.5 x 10^7 m^{-2} , 5.8 x 10^7 m^{-2} , and 5.8 x 10^7 m^{-2} for INP at -20, -25, and -30 °C. The lack of a significant difference in the median value of n_s between -25 and -30 °C may again be due to the fact that the CFDC-IAS was periodically ran only at -30 °C for several days in a row, and these days included some of the lowest INP concentrations of the campaign. The median n_s values more closely follow the fit to clean marine data found by (McCluskey et al., 2018) than the fit for dust INP found by (Ullrich et al., 2017). Our data also falls within n_s ranges for some species of pollens (Murray et al., 2012). Less than 1% of calculated n_s values reached above 10^9 m^{-2}. These higher values have been found to be indicative of dust, or mineral INPs (Murray et al., 2012), potentially indicating that INP during the winter at SPL are dominated by species other than dust or mineral particles.

We also calculate the parameterizations laid out in (Niemand et al., 2012; DeMott et al., 2010, 2015), hereon D10 and D15, that relate aerosol concentrations > 500 nm to INP concentrations as a function of activation temperature (Figure 5). D10 was constructed for "global" (unspeciated) INP while available coefficient values for D15 parameterization are applicable for mineral dusts. D10 was found in (Niemand et al., 2012; DeMott et al., 2010, 2015) to reduce variability in INP at a given temperature to less than a factor of 10. While 86% of the predicted INP concentrations lie within the 1:10 and 10:1 lines (green dashed line, Figure 5), 13.8% of data lie between the 1:10 and 1:100 lines (orange dot-dash line, Figure 5) and 0.2% of data falls outside of the 1:100 line. Similarly, the D15 parameterization captures 70.4% of data within the 1:10 and 10:1 lines, with 19.7% falling between the 1:10 and 1:100 line and 9.9% of data falling outside of the 1:100 line. In general, both parameterizations perform best for the coldest (-30 °C) data but tend to underpredict observed INP concentrations, similar to findings of (Bi et al., 2019).

4. Conclusions

The established Continuous Diffusion Flow Chamber (CFDC) has an excellent track record of providing high-resolution ice nucleating particle (INP) measurements but has traditionally required an on-site, trained technician to run. Significant automation updates to the CFDC design to create the CFDC-Ice Activation Spectrometer (CFDC-IAS) allow for near continuous operation with minimal user intervention. We have deployed the CFDC-IAS at Storm Peak Laboratory (SPL), a long-term, mountain measurement site in Steamboat Springs, Colorado, USA for four months (October 2020-January 2021) to gather a high-resolution dataset of INP. This public dataset may be of interest for more in-depth scientific analyses beyond the general overview provided here and model-measurement comparison. We cycled between target temperatures of -20, -25,

https://doi.org/10.5194/amt-2022-216
Preprint. Discussion started: 20 July 2022


Atmospheric Measurement Techniques Discussions

and -30 °C for each measurement period, achieving stable conditions throughout the campaign. Concentrations of INPs were typically around a median of 6 sL^{-1} , mean of 10 sL^{-1} at all temperature ranges, similar to previous CFDC measurements at SPL taken during fall and spring of 2001 and 2004, respectively (Richardson et al., 2007; DeMott et al., 2003). However, our measurements captured a higher range of INP (~0-470 sL^{-1}) than these earlier campaigns. The higher temporal coverage of our measurements compared to the earlier campaigns increase our ability to capture short-term, high-concentration events. As well, there may be different transport patterns or ambient conditions between this and previous campaigns. Our deployment of the CFDC-IAS at SPL provides promise for its potential for future longer deployments to help build up much-needed long-term, high-resolution INP datasets.

Data availability

The CFDC-IAS data is available at https://handixscientific.synology.me:8115/fsdownload/HYkyi0dOM/External.

Author contributions

ALH performed the data analysis and wrote the manuscript with assistance from EJTL, GRM, AGH, and CNR. EJTL, GRM, DRG, IM, CNR, and AGH performed or oversaw SPL measurements used in this manuscript.

Acknowledgements

Development and deployment of the CFDC-IAS was supported in part by NASA SBIR Contract 80NSSC19C0166. The NSF Atmospheric Chemistry Program provided support (Grant # AGS-2025215).

References

Amin, H., Atkins, P. T., Russo, R. S., Brown, A. W., Sive, B., Hallar, A. G., and Huff Hartz, K. E.: Effect of bark beetle infestation on secondary organic aerosol precursor emissions, Environ. Sci. Technol., 46, 5696–5703, 2012.

Amin, H. S., Russo, R. S., Sive, B., Richard Hoebeke, E., Dodson, C., McCubbin, I. B., Gannet Hallar, A., and Huff Hartz, K. E.: Monoterpene emissions from bark beetle infested Engelmann spruce trees, Atmos. Environ., 72, 130–133, 2013.

Barry, K. R., Hill, T. C. J., Levin, E. J. T., Twohy, C. H., Moore, K. A., Weller, Z. D., Toohey, D. W., Reeves, M., Campos, T., Geiss, R., Schill, G. P., Fischer, E. V., Kreidenweis, S. M., and DeMott, P. J.: Observations of ice nucleating particles in the free troposphere from western US wildfires, J. Geophys. Res., 126, https://doi.org/10.1029/2020jd033752, 2021.

Bigg, E. K.: Ice Nucleus Concentrations in Remote Areas, J. Atmos. Sci., 30, 1153–1157, 1973.

Bigg, E. K. and Miles, G. T.: The Results of Large–Scale Measurements of Natural Ice Nuclei, J. Atmos. Sci., 21, 396–403, 1964.

Bi, K., McMeeking, G. R., Ding, D. P., Levin, E. J. T., DeMott, P. J., Zhao, D. L., Wang, F., Liu, Q., Tian, P., Ma, X. C., Chen, Y. B., Huang, M. Y., Zhang, H. L., Gordon, T. D., and Chen, P.: Measurements of ice nucleating particles in Beijing, China, J. Geophys. Res., 124, 8065–8075, 2019.

https://doi.org/10.5194/amt-2022-216
Preprint. Discussion started: 20 July 2022

Borys, R. D. and Wetzel, M. A.: Storm Peak Laboratory: A Research, Teaching, and Service Facility for the Atmospheric Sciences, https://doi.org/10.1175/1520-0477(1997)078<2115:splart>2.0.co;2, 1997.

Boucher, O., Randall, D., Artaxo, P., and Bretherton, C.: Clouds and aerosols, 2013.

Connolly, P. J., Möhler, O., Field, P. R., Saathoff, H., Burgess, R., Choularton, T., and Gallagher, M.: Studies of heterogeneous freezing by three different desert dust samples, Atmos. Chem. Phys., 9, 2805–2824, 2009.

DeCarlo, P., Slowik, J., Worsnop, D., Davidovits, P., and Jimenez, J.: Particle Morphology and Density Characterization by Combined Mobility and Aerodynamic Diameter Measurements. Part 1: Theory, https://doi.org/10.1080/02786826.2004.10399461, 2004.

DeMott, P. J., Cziczo, D. J., Prenni, A. J., Murphy, D. M., Kreidenweis, S. M., Thomson, D. S., Borys, R., and Rogers, D. C.: Measurements of the concentration and composition of nuclei for cirrus formation, Proc. Natl. Acad. Sci. U. S. A., 100, 14655–14660, 2003.

DeMott, P. J., Prenni, A. J., Liu, X., Kreidenweis, S. M., Petters, M. D., Twohy, C. H., Richardson, M. S., Eidhammer, T., and Rogers, D. C.: Predicting global atmospheric ice nuclei distributions and their impacts on climate, Proc. Natl. Acad. Sci. U. S. A., 107, 11217–11222, 2010.

DeMott, P. J., Prenni, A. J., McMeeking, G. R., Sullivan, R. C., Petters, M. D., Tobo, Y., Niemand, M., Möhler, O., Snider, J. R., Wang, Z., and Others: Integrating laboratory and field data to quantify the immersion freezing ice nucleation activity of mineral dust particles, Atmos. Chem. Phys., 15, 393–409, 2015.

DeMott, P. J., Hill, T. C. J., Petters, M. D., Bertram, A. K., Tobo, Y., Mason, R. H., Suski, K. J., McCluskey, C. S., Levin, E. J. T., Schill, G. P., and Others: Comparative measurements of ambient atmospheric concentrations of ice nucleating particles using multiple immersion freezing methods and a continuous flow diffusion chamber, Atmos. Chem. Phys., 17, 11227–11245, 2017.

Draxler, R. R. and Hess, G. D.: Description of the HYSPLIT4 modeling system, 1997.

Draxler, R. R. and Hess, G. D.: An overview of the HYSPLIT_4 modelling system for trajectories, Aust. Meteorol. Mag., 47, 295–308, 1998.

Garimella, S., Kristensen, T. B., Ignatius, K., Welti, A., Voigtländer, J., Kulkarni, G. R., Sagan, F., Kok, G. L., Dorsey, J., Nichman, L., Rothenberg, D. A., Rösch, M., Kirchgäßner, A. C. R., Ladkin, R., Wex, H., Wilson, T. W., Ladino, L. A., Abbatt, J. P. D., Stetzer, O., Lohmann, U., Stratmann, F., and Cziczo, D. J.: The SPectrometer for Ice Nuclei (SPIN): an instrument to investigate ice nucleation, https://doi.org/10.5194/amt-9-2781-2016, 2016.

Hallar, A. G., Gannet Hallar, A., Chirokova, G., McCubbin, I., Painter, T. H., Wiedinmyer, C., and Dodson, C.: Atmospheric bioaerosols transported via dust storms in the western United States, https://doi.org/10.1029/2011gl048166, 2011.

Hallar, A. G., Petersen, R., Mccubbin, I. B., Lowenthal, D., Lee, S., Andrews, E., and Yu, F.: Climatology of New Particle Formation and Corresponding Precursors at Storm Peak Laboratory, 16, 816–826, 2016.

Kline, D. B.: EVIDENCE OF GEOGRAPHICAL DIFFERENCES IN ICE NUCLEI CONCENTRATIONS, Mon. Weather Rev., 91, 681–686, 1963.

Lacher, L., DeMott, P. J., Levin, E. J. T., Suski, K. J., Boose, Y., Zipori, A., Herrmann, E., Bukowiecki, N., Steinbacher, M., Gute, E., Abbatt, J. P. D., Lohmann, U., and Kanji, Z. A.: Background free-tropospheric ice nucleating particle concentrations at mixed-phase cloud conditions, J. Geophys. Res., 123, 10,506–10,525, 2018.

https://doi.org/10.5194/amt-2022-216
Preprint. Discussion started: 20 July 2022


Atmospheric Measurement Techniques Discussions

Levin, E. J. T., DeMott, P. J., Suski, K. J., Boose, Y., Hill, T. C. J., McCluskey, C. S., Schill, G. P., Rocci, K., Al-Mashat, H., Kristensen, L. J., Cornwell, G., Prather, K., Tomlinson, J., Mei, F., Hubbe, J., Pekour, M., Sullivan, R., Leung, L. R., and Kreidenweis, S. M.: Characteristics of ice nucleating particles in and around California winter storms, J. Geophys. Res., 124, 11530–11551, 2019.

McCluskey, C. S., Ovadnevaite, J., Rinaldi, M., Atkinson, J., Belosi, F., Ceburnis, D., Marullo, S., Hill, T. C. J., Lohmann, U., Kanji, Z. A., O'Dowd, C., Kreidenweis, S. M., and DeMott, P. J.: Marine and Terrestrial Organic Ice-Nucleating Particles in Pristine Marine to Continentally Influenced Northeast Atlantic Air Masses, J. Geophys. Res. Atmos. , https://doi.org/10.1029/2017jd028033, 2018.

MesoWest, https://mesowest.utah.edu/, last access: 12 January, 2022.

Müller, W.: Influence of different meteorological conditions on the concentration of freezing nuclei, 18, 55, 1969a.

Müller, W.: Über den Einfluß meteorologischer Bedingungen auf die Gefrierkerndichte der Luft, Arch. Met. Geoph. Biokl. A., 18, 55–74, 1969b.

Murray, B. J., O'Sullivan, D., Atkinson, J. D., and Webb, M. E.: Ice nucleation by particles immersed in supercooled cloud droplets, Chem. Soc. Rev., 41, 6519–6554, 2012.

Ng, N. L., Herndon, S. C., Trimborn, A., Canagaratna, M. R., Croteau, P. L., Onasch, T. B., Sueper, D., Worsnop, D. R., Zhang, Q., Sun, Y. L., and Jayne, J. T.: An Aerosol Chemical Speciation Monitor (ACSM) for Routine Monitoring of the Composition and Mass Concentrations of Ambient Aerosol, Aerosol Sci. Technol., 45, 780–794, 2011.

Niemand, M., Möhler, O., Vogel, B., Vogel, H., Hoose, C., Connolly, P., Klein, H., Bingemer, H., DeMott, P., Skrotzki, J., and Leisner, T.: A Particle-Surface-Area-Based Parameterization of Immersion Freezing on Desert Dust Particles, J. Atmos. Sci., 69, 3077–3092, 2012.

Obrist, D., Hallar, A. G., McCubbin, I., Stephens, B. B., and Rahn, T.: Atmospheric mercury concentrations at Storm Peak Laboratory in the Rocky Mountains: Evidence for long-range transport from Asia, boundary layer contributions, and plant mercury uptake, Atmos. Environ., 42, 7579–7589, 2008.

Petersen, R. C., Hallar, A. G., McCubbin, I. B., Ogren, J. A., Andrews, E., Lowenthal, D., Gorder, R., Purcell, R., Sleeth, D., and Novosselov, I.: Numerical, wind-tunnel, and atmospheric evaluation of a turbulent ground-based inlet sampling system, Aerosol Sci. Technol., 53, 712–727, 2019.

Richardson, M. S., DeMott, P. J., Kreidenweis, S. M., Cziczo, D. J., Dunlea, E. J., Jimenez, J. L., Thomson, D. S., Ashbaugh, L. L., Borys, R. D., Westphal, D. L., Casuccio, G. S., and Lersch, T. L.: Measurements of heterogeneous ice nuclei in the western United States in springtime and their relation to aerosol characteristics, J. Geophys. Res., 112, https://doi.org/10.1029/2006jd007500, 2007.

Rogers, D. C., DeMott, P. J., Kreidenweis, S. M., and Chen, Y.: A Continuous-Flow Diffusion Chamber for Airborne Measurements of Ice Nuclei, https://doi.org/10.1175/1520-0426(2001)018<0725:acfdcf>2.0.co;2, 2001.

Rolph, G., Stein, A., and Stunder, B.: Real-time Environmental Applications and Display sYstem: READY, 95, 210–228, 2017.

Schneider, J., Höhler, K., Heikkilä, P., Keskinen, J., Bertozzi, B., Bogert, P., Schorr, T., Umo, N. S., Vogel, F., Brasseur, Z., and Others: The seasonal cycle of ice-nucleating particles linked to the abundance of biogenic aerosol in boreal forests, Atmos. Chem. Phys., 21, 3899–3918, 2021.

https://doi.org/10.5194/amt-2022-216
Preprint. Discussion started: 20 July 2022

Atmospheric Measurement Techniques Discussions

Schrod, J., Kleinhenz, D., Hörhold, M., Erhardt, T., Richter, S., Wilhelms, F., Fischer, H., Ebert, M., Twarloh, B., Della Lunga, D., and Others: Ice-nucleating particle concentrations of the past: insights from a 600-year-old Greenland ice core, Atmos. Chem. Phys., 20, 12459–12482, 2020a.

Schrod, J., Thomson, E. S., Weber, D., Kossmann, J., Pöhlker, C., Saturno, J., Ditas, F., Artaxo, P., Clouard, V., Saurel, J.-M., and Others: Long-term deposition and condensation ice-nucleating particle measurements from four stations across the globe, Atmos. Chem. Phys., 20, 15983–16006, 2020b.

Soulage, G.: Counting and electron microscope study of European ice nuclei, 1966.

Steamboat Springs, CO (057936), https://wrcc.dri.edu/cgi-bin/cliMAIN.pl?co7936, last access: 12 January, 2022.

Stein, A. F., Draxler, R. R., Rolph, G. D., Stunder, B. J. B., Cohen, M. D., and Ngan, F.: NOAA's HYSPLIT atmospheric transport and dispersion modeling system, Bull. Am. Meteorol. Soc., 96, 2059–2077, 2015.

Ullrich, R., Hoose, C., Möhler, O., Niemand, M., Wagner, R., Höhler, K., Hiranuma, N., Saathoff, H., and Leisner, T.: A New Ice Nucleation Active Site Parameterization for Desert Dust and Soot, J. Atmos. Sci., 74, 699–717, 2017.

U.S. Drought Monitor, https://droughtmonitor.unl.edu/Maps/MapArchive.aspx, last access: 12 January 2022.

https://doi.org/10.5194/amt-2022-216
Preprint. Discussion started: 20 July 2022

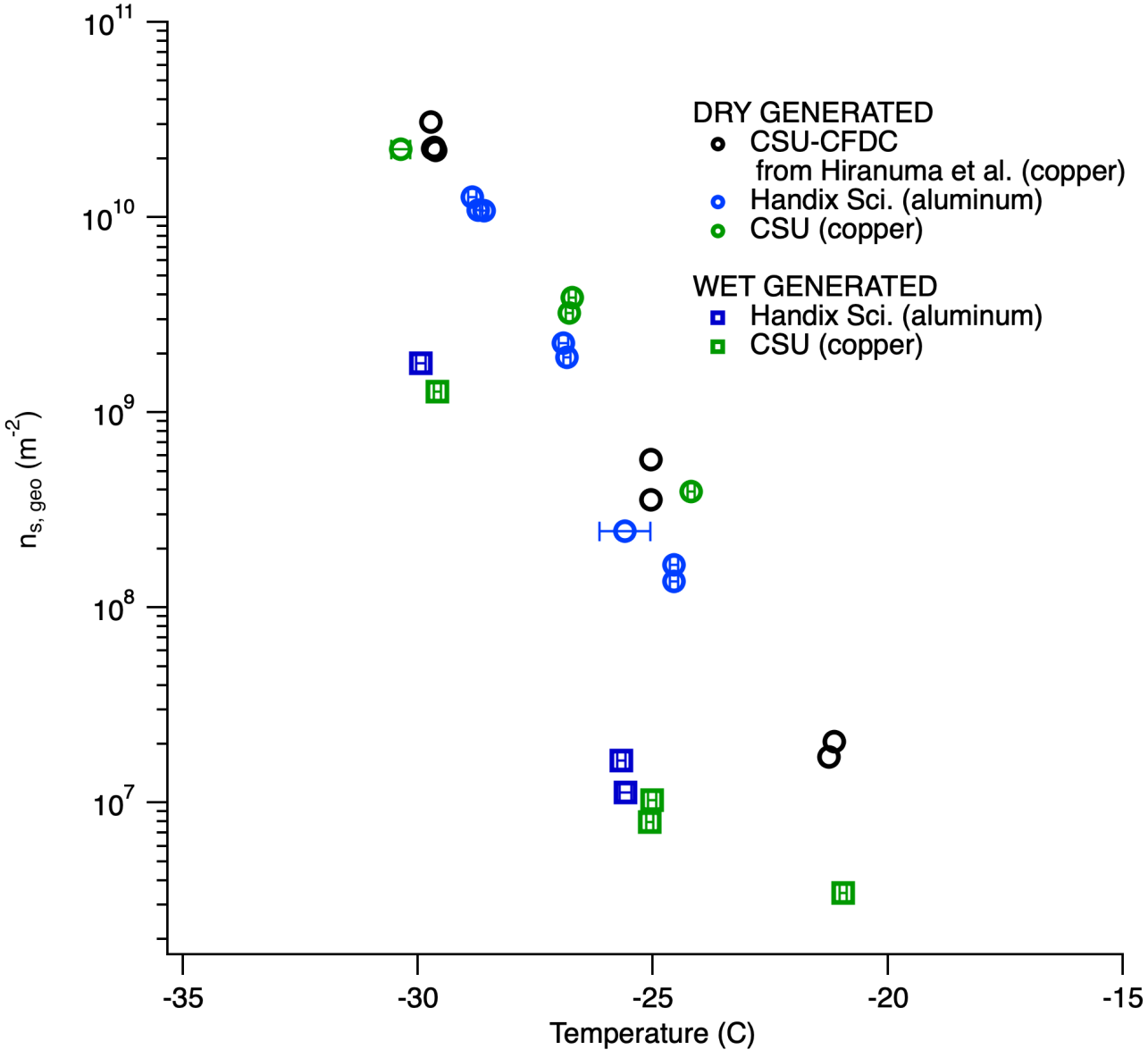

Figure 1: Active site density (ns) calculated for 500 nm illite particles generated using a nebulizer (wet; squares) or dry (circles) from CFDC measurements. Green points show measurements made with the CSU CFDC, which uses a copper column, blue points indicate data from the aluminum column CFDC-IAS. Black points show literature data from the CSU CFDC. The x-axis error bars indicate the +/- one standard deviation in temperature measured during the measurement interval (approximately 5 minutes).

https://doi.org/10.5194/amt-2022-216
Preprint. Discussion started: 20 July 2022

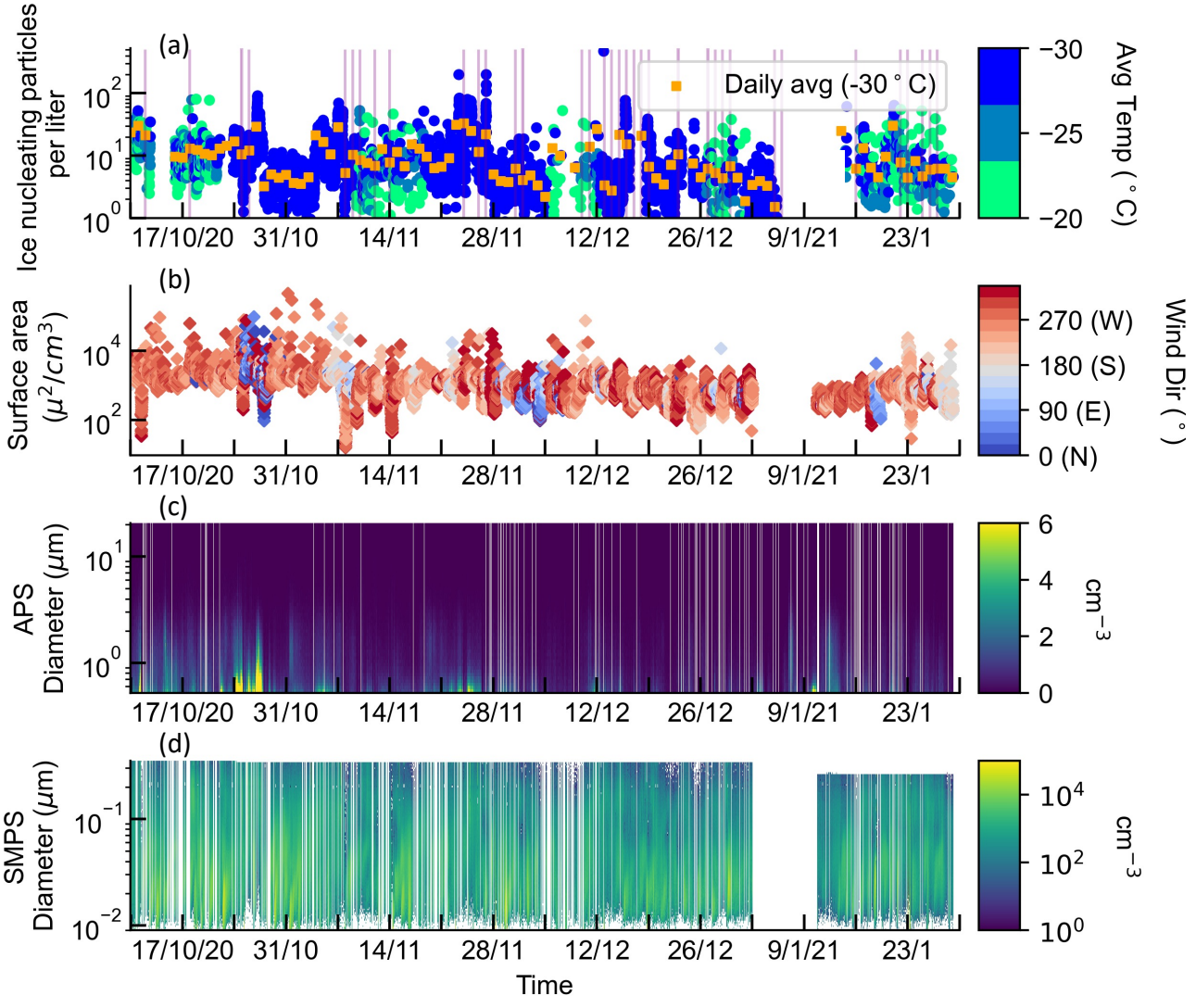

Figure 2. (a) Time series of ice nucleating particles (INP) colored by the average temperature of the CFDC observed at Storm Peak Laboratory (SPL) between October 2020-January 2021 (MST) and daily average INP at -30 C° (orange points). Precipitation event days are marked with purple horizontal lines. (b) Calculated particle surface area between 10 nm - 2.5 µm, colored by wind direction in degrees, where 0° is north and 270° is west. The wind direction is discretized by cardinal direction. (c) Time series of hourly aerodynamic particle sizer (APS) data observed at SPL. (d) Time series of hourly scanning mobility particle sizer (SMPS) data observed at SPL for the same time period.

https://doi.org/10.5194/amt-2022-216
Preprint. Discussion started: 20 July 2022

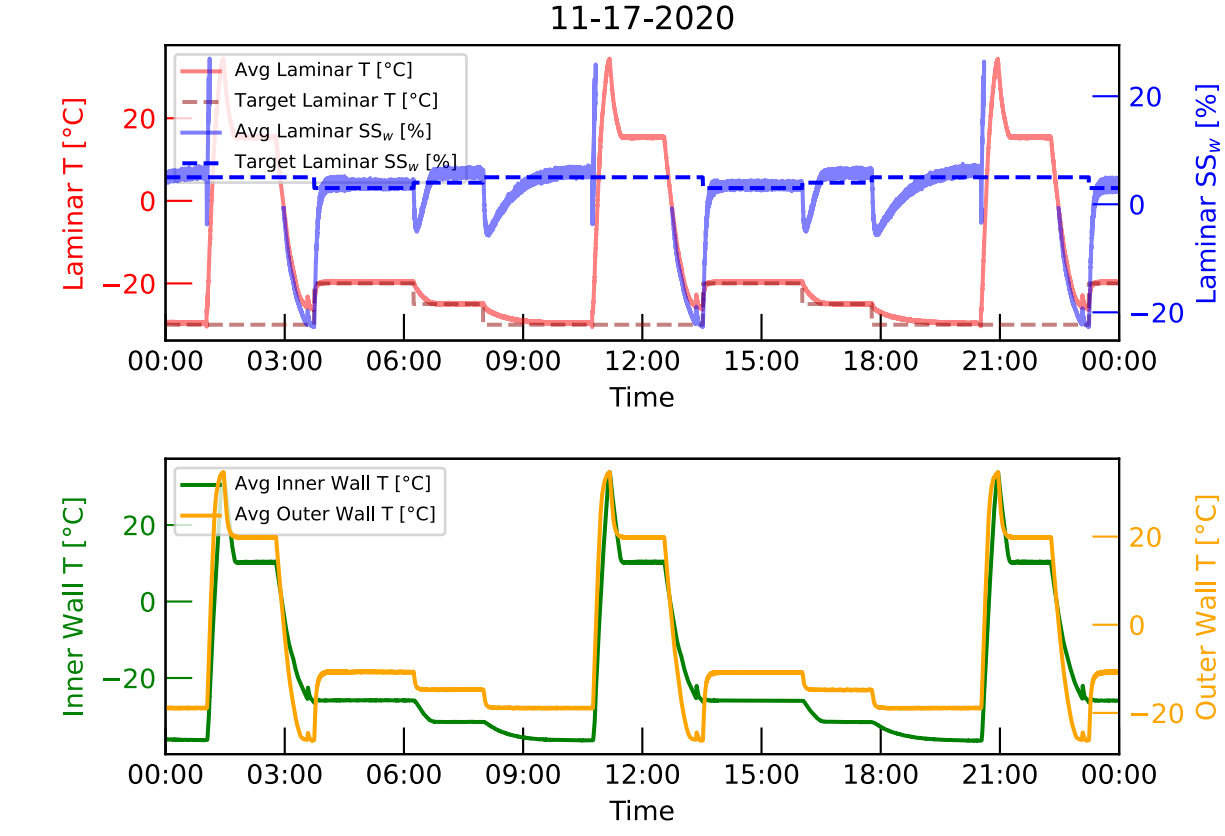

Figure 3. Example of CFDC-IAS operating conditions for November 17, 2020, in local time (MST). (Top) Target and average laminar temperatures in C (left axis) and target and average water supersaturations in % (right axis). (Bottom) Average inner wall temperature (left axis) and outer wall temperature (right axis) in C.

https://doi.org/10.5194/amt-2022-216
Preprint. Discussion started: 20 July 2022

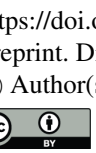

Atmospheric Measurement Techniques Discussions

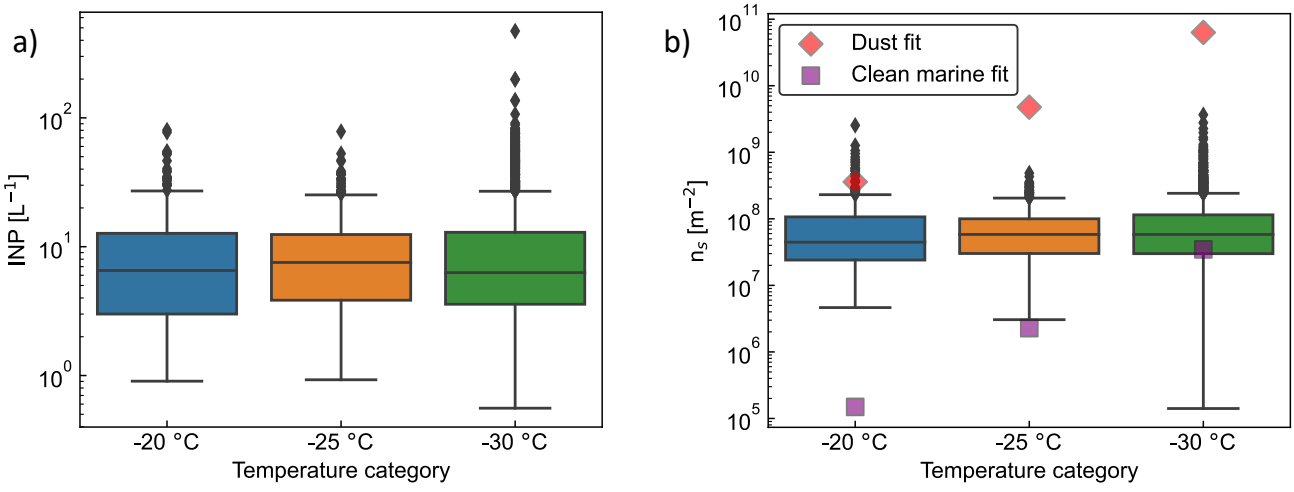

Figure 4. a) All statistically significant INP observed at Storm Peak Laboratory, by temperature range. The number of samples (N) for each boxplot is N=385 for -20 °C, N=445 for -25 °C , and N= 2993 for -30 °C. b) Surface active site density, n_s, using aerosol surface area from the SMPS and APS. The dust fit is from Ullrich et al., (2017) (their equation 5) and McCluskey et al. (2018) (outlined in their Sect. 3.5). The number of samples (N) for each boxplot is N=314 for -20 °C, N=380 for -25 °C , and N= 2453 for -30 °C.

https://doi.org/10.5194/amt-2022-216
Preprint. Discussion started: 20 July 2022

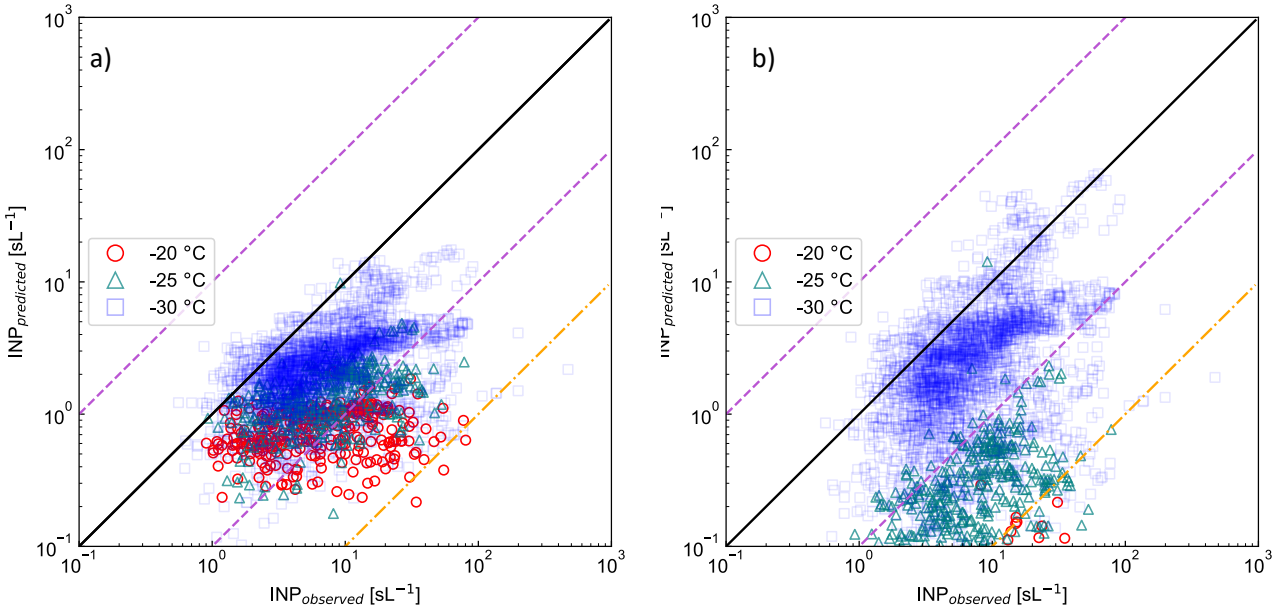

Figure 5. a) The "D10" (Demott et al., 2010) parameterization. b) The "D15" (Demott et al., 2015) parameterization. The black solid lines on both subplots are the 1-to-1 line, the purple dashed lines are the 1-to-10 and 10-to-1 lines, and the orange dashed lines are the 1-to-100 lines.